FLOMEKO2019
18th International Flow Measurement Conference
Portugal | Lisbon | LNEC | 26-28 june 2019

Turbulence Measurements With A New Two Components Ultrasonic Profiler

H. Guta[1], S. Fischer[2], D. Dufour[2], M. Burckbuchler[2], G. Fromant[1]

[1] Laboratory of Geophysical and Industrial Flows, Grenoble, France
[2]UBERTONE, Strasbourg, France, info@ubertone.fr
E-mail (corresponding author): marie@ubertone.fr

Abstract

In the present paper, a data set of time-resolved two components velocity profile measurements under steady uniform turbulent rough clear water and sheet-flow are presented. The purpose of this campaign was to evaluate the performances of a commercial ADVP, the *UB-Lab 2C* from the company Ubertone, by comparing it to a well-established instrument, the ACVP, developed by the LEGI. This measurement method provides quasi-instantaneous co-located two (2C) components velocity profiles, overcoming limitations of previously developed acoustic measurement methods, and allowing to resolve fine flow scale for the characterisation of turbulence statistics and turbulent processes.
Taking into account flow condition differences in the tilting flume with sediment pit, the results of this measurement campaign demonstrates the good performance of the commercial ADVP compared to the ACVP, in clear water and sheet-flow. Its capabilities for time-resolved turbulence measurements are also supported by similar results described in the literature, namely, the significant reduction of Von Karman parameter in sediment-laden flows and the higher contributions of ejections in CW (and sweeps in SF) for the Reynolds shear stress. This suggests the potential of this acoustic system to analyse a wide range of hydrodynamic phenomena, both in rigid-bed and mobile-bed, in which turbulence plays a major role.

1. Introduction

Measuring velocity profiles in turbulent flows has always been of great theoretical and practical interest. It allows the statistical characterisation of turbulence and better understanding of processes such as sediment motion, closely related to the flow turbulence. A full agreement on how turbulent flows are affected by presence of particles is yet to be reached. An example is the modification of the well-known law of the wall, which has been the subject of analysis by several authors ([4], [14], [16]). All the studies report a reduction of the von Karman parameter in mobile-bed flows, however, the full description of these modifications according to the sediment-laden flow regime is not available. Another question lies in understanding the behaviour of turbulent bursting events. They are reported ([18], [13], [11], [5]) to be very important on the suspension dynamics.

Over the past two decades, the development of increasingly sophisticated measuring systems has enabled flow parameters to be obtained from acoustic technology. For example Acoustic Doppler Current Profilers (divergent beams on a multi-monostatic configuration) or UVPs (single (1C) and multi-components velocity profilers), are able of reasonable to high temporal and spatial resolutions and have been increasingly used in the fields of research and environmental engineering. Yet, none of these devices allow to resolve sufficiently fine flow scales, preventing a proper characterization of turbulence statistics and turbulent processes. To overcome these limitations, ADVPs (Acoustic Doppler Velocity Profilers) were developed to provide quasi-instantaneous co-located two (2C) to three (3C) components velocity profiles along the transmitter beam axis, using a multi-bistatic configuration. These devices were shown to resolve up to the Taylor microscale.

The study aims to display the performance of the UB-MES (a prototype of the *UB-Lab 2C* currently commercialised) in terms of mean flow properties and time-resolved turbulence measurements, focusing in the von Karman and turbulent bursting events modifications in sheet-flow.

The structure of the paper is as follows: in section 2 the experimental setup and flow conditions are presented. The mean flow properties and time-resolved turbulence

measurement results in clear water are presented and discussed in section 3. In section 4, the sheet flow results are presented. The turbulence measurement capabilities of UB-MES are summarised in section 5.

2. Methodology

2.1 Experimental setup

The experiments were carried out at the LEGI, using a 10 m long tilting flume, with 0.35 m width. Different slopes were set for clear water experiments and for sheet-flow experiments. For sheet flow experiments, the (rectangular) sediment pit, located at 5 m from the beginning of the channel is 3 x 0.11 m2, is initially filled with low density (ρv=1192 kg/m3) non-spherical plastic sediments (Poly-Methyl MethAcrylate) of median diameter d_p=3 mm and the packed volumetric concentration is 0.55. The settling velocity w_s of the particles is 5.6 cm/s. The fixed bed is covered by glued particles, with the same properties as the sediments filled in the channel. For the clear water measurements, the fixed bed is placed in the sediment pit. For both conditions (clear water and sheet flow), a sluice gate at the downstream end and a by-pass at the upstream end allow to regulate the flow discharge.

2.2 Experimental protocol and flow properties

The sheet-flow experimental protocol from [16] was applied. The experiments are performed with no recirculation of the sediments. In such conditions, there is an initial transient phase, in which the bed erosion rate reaches its peak value, followed by a quasi-uniform phase of the flow, with a fairly steady bed erosion rate, which lasts about 30 s. The flow analysis is performed during this quasi-steady period, in which the flow is quasi-uniform. For better statistical convergence, the flow quantities are averaged over 4 experimental runs with ACVP and 5 experimental runs with UB-MES.

For clear water experiments, no particular protocol was implemented since the sediment pit was covered by fixed rough bed plates. It was only necessary to approach the uniform flow conditions for which the mean flow and turbulence properties are well known and described in the literature [13].

For both clear water and sheet-flow conditions, the flow was highly turbulent, hydraulically rough and subcritical (Table 1), as indicated by the high Reynolds number ($Re = UH_f/\nu > 2000$), the high bed roughness Reynolds number ($Re^* = u\, k_s/\nu > 70$) and the low Froude number ($Fr = U/\sqrt{(g\, H_f)} < 1$).

Table 1: Sediment and flow properties in Clear water (CW) and Sheet-flow (SF) & UB-MES)

	S_0 (%)	u_* (cm/s)	H_f (m)	Q (m^3/s)	U (m/s)	Re $(-)$	Fr (-)
$CW_{(ACVP}$	0.375	5.7	0.12	28,9	0.69	8×10^4	0.6
$SF_{(ACVP)}$	0.5	4.3	0.135	28.8	0.59	8×10^4	0.5
$SF_{(UB-MES)}$	0.5	4.1	0.145	28.8	0.55	8×10^4	0.5

S_0: Slope of the channel; U: bulk mean velocity; H_f: water depth; ν: kinematic viscosity of water; u_*: friction velocity; k_s: equivalent roughness (k_s=2.5 d_p for mobile bed experiments and k_s=3 mm for clear water) and g is the gravitational acceleration.

2.3 ACVP and UB-MES

Several authors ([8], [7], [10], [16], [17], [3]) have successfully performed velocity, concentration and sediment flux measurements using the ACVP, and compared it to other measurement techniques.

The company Ubertone has recently developed a commercial version of the ACVP: the *UB-Lab 2C* whose prototype is named UB-MES in this paper. One of the major differences between the two systems is that, unlike the ACVP, the UB-MES is compact, low power and the embedded software runs autonomously. Consequently, it is limited in terms of continuous data flow load in opposition with the ACVP. For both acoustic systems, the carrier frequency was set to 1 MHz, with a pulse duration of 2 µs allowing a vertical spatial resolution of 1.5 mm. The obtained time resolution for velocity measurements was 19 Hz.

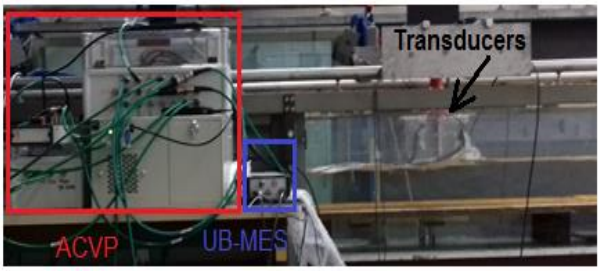

Figure 1: Illustration of UB-MES (blue) and ACVP (red).

Figure 1 shows UB-MES prototype and ACVP. The same set of transducers was used with both systems, in order to compare the functioning of the systems solely in terms of electronics. It is possible to see that UB-MES is significantly compact in comparison with ACVP. This gives UB-MES an important advantage in terms of mobility. In contrast, for high time-space resolutions, ACVP provides a larger vertical profiling range.

2.4. Velocity measurement principle

The velocity profiling principle in both acoustic systems relies on the measurement of Doppler frequencies. By employing one emitter (that emits sound pulses at a given frequency) and two receivers (Figure 2), two Doppler frequencies along the common emitter axis can be measured. The streamwise velocity u and the flow normal velocity w are then obtained from the Doppler Shift frequencies (Equation 1 and 2)

$$u = \frac{c}{2f_0 sin\alpha}(f_d{}^+ - f_d{}^-) \quad (1)$$

$$w = \frac{c}{2f_0(1+cos\,\alpha)}(f_d{}^+ + f_d{}^-) \quad (2)$$

where $f_d{}^+$ and $f_d{}^-$ are the Doppler frequencies obtained from the two receivers, f_0 is the emitted frequency, c is the sound speed in water and α is the angle between the emitter and receiver axis. The echo intensities are backscattered by air bubbles contained in the fluid, and by the suspended particles in case of sheet-flow.

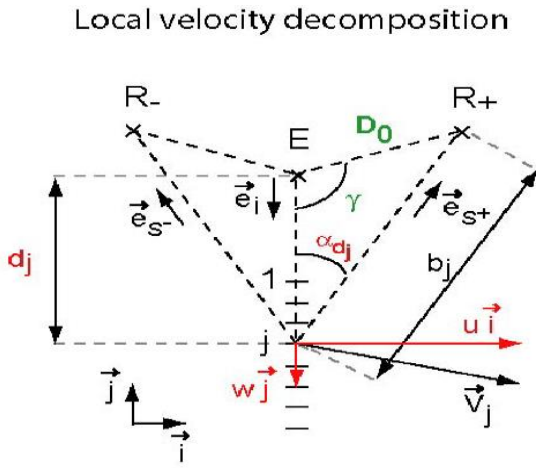

Figure 2: Configuration of the transducers, with one emitter E and two receivers R- and R+ R.

3. Results and Discussion - Clear Water (CW)

The first part of the analysis determines the fluid velocity measurement performances of the UB-MES prototype in terms of mean quantity and its fluctuations.

3.1 Mean velocity and velocity fluctuations

Figure 2 presents the streamwise mean velocity profiles measured by the ACVP and the UB-MES as functions of the bottom distance normalized by the water flow depth *Hf*.

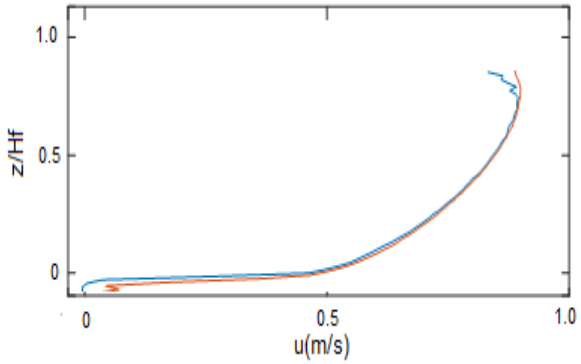

Figure 2: Mean velocity profile for UB-MES (blue) and ACVP(red)

As observed in Figure 2 the mean velocity profiles measured by ACVP and UB-MES under the same clear water flow conditions are in good agreement. In both systems, it can be found the typical logarithmic behaviour of the velocity profile. In the upper region of the flow, the flow is strongly disturbed by the presence of the box holding the sensors positioned at the free-surface height. In the near bed there is the effect of the rough sublayer.

The degree of velocity fluctuations generated by turbulent eddies can be described by turbulence intensities. Figure 3 shows the turbulence intensity profiles for the horizontal (u) and vertical (w) components as a function of the (normalized) distance to the wall. There is a very good agreement between the UB-MES and ACVP measurements on the entire vertical profile. The origin of the discrepancies in the near-bed and the upper region of the flow referred previously for the mean velocity measurements are also valid for turbulence intensities. The normalized mean turbulent intensities can be defined as:

$$u_{rms} = \frac{\sqrt{\overline{u'^2}}}{u_*} \quad (3)$$

$$w_{rms} = \frac{\sqrt{\overline{u'^2}}}{u_*} \quad (4)$$

where $\overline{u'}$ and $\overline{w'}$ denote the mean streamwise and the vertical velocity fluctuations, respectively. The measurements of turbulent intensities obtained by the two instruments reveal the same degree of anisotropy between the horizontal and vertical components, which is induced by the average friction exerted by the flow on the rigid rough bottom (sheared boundary layer on rough wall).

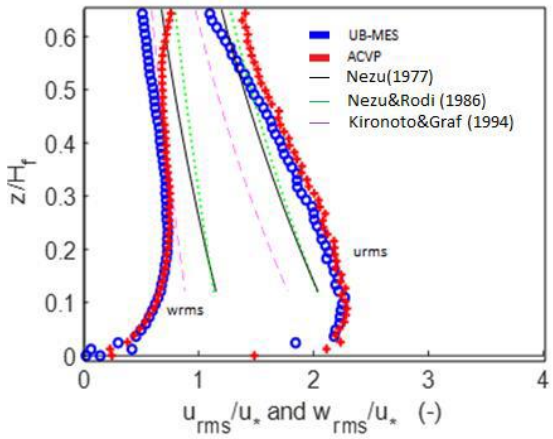

Figure 3: Normalized mean turbulence intensity profiles.

The values of the normalized intensities as well as the shapes of the associated profiles (Figure 4) are very similar to those found in the literature for rough open channel turbulent flows ([12], [13]), which can be estimated by the following formulas:

$$\frac{u_{rms}}{u_*} = Bu\ exp(-C_u z) \quad (5)$$

$$\frac{w_{rms}}{w_*} = Bw\ exp(-C_u z) \quad (6)$$

where the empirical parameters B_u, B_w, C_u and C_w have been proposed by several authors, and the resulting turbulence intensities are presented in Figure 3.

The mean relative differences between the measurements of mean velocity profiles and turbulence intensities with both systems are below 10%.

3.2 Turbulent bursting events

Turbulent bursting phenomenon and the resulting coherent structures are relevant in understating sediment entrainment process in turbulent flows. Turbulent bursting events can be quantified from conditional statistics of velocity fluctuations ([13], [6], [17]).

This procedure allows to evaluate the total Reynolds shear stress at a given point as a sum of contributions from different bursting events, which are distinguished according to the quadrant in plane [9], and the respective threshold level H: outward interactions, ejections inward interactions and sweeps. The analysis of conditional statistics consists in fixing a threshold level that allows to exclude weak events (below the magnitude defined by the threshold level H).

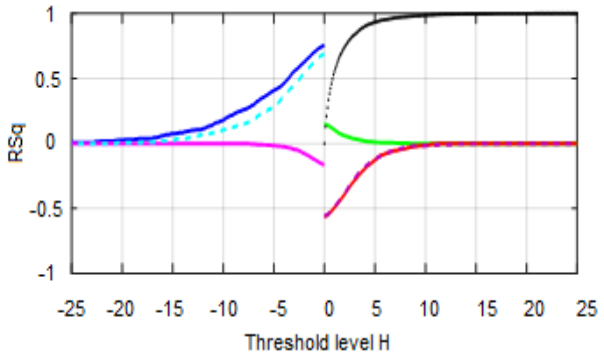

Figure 4: Quadrant threshold distribution of fractional contributions (RSq) to turbulent shear stress, at z/Hf=0.3, for UB-MES (solid lines) and for ACVP (dashed lines). blue=Sweeps, red=Ejections, green=Outward interactions and purple=Inward interactions.

Figure 4 displays the quadrant threshold distribution, in terms of fractional contribution (RSq) to the total Reynolds shear stress of different events (in colors), at a given vertical position (z/Hf=0.30), as function of the threshold level H, for UB-MES (solid lines) and ACVP (dashed lines). The black line represents the proportion of events with lower magnitude than the magnitude at threshold level. As the threshold increases, only the stronger events are selected, thus the reduction in fractional contributions and an increase of excluded events is observed. It should be noted that from a given threshold level (H~5) only ejections and sweeps contribute for total Reynolds shear stress. Additionally, it can be observed that ejections are the bursting events with higher magnitude. As result, from the threshold level H~10, only ejections are responsible for the Reynolds shear stress. This is true for both systems. These results are consistent with the literature ([13], [2]), who reported ejections as the main contributors to the turbulent shear stress in rigid-bed turbulent flows.

4. Results and Discussion – Sheet Flow (SF)

In this section, firstly, the mean velocity and mean turbulent shear stress, which result from streamwise and vertical velocity fluctuations in both systems are compared. Secondly, comparisons (in terms of von Karman parameter and turbulent bursting phenomenon) with clear water are established. The corresponding Shields number θ was about 0.3 for both systems. The suspension number is w_s/u^*=1.4 and 1.3 for UB-MES and ACVP respectively.

4.1 Mean velocity and mean Reynolds shear stress profiles

Figure 5a displays the mean streamwise velocity profiles for ACVP (+) and UB-MES (o). The relative difference between UB-MES and ACVP increased with elevation up to 14% at the top of the profiles. Such

difference is attributed to different flow conditions, despite the same flow regime, as indicated by the same order of magnitude of the flow parameters.

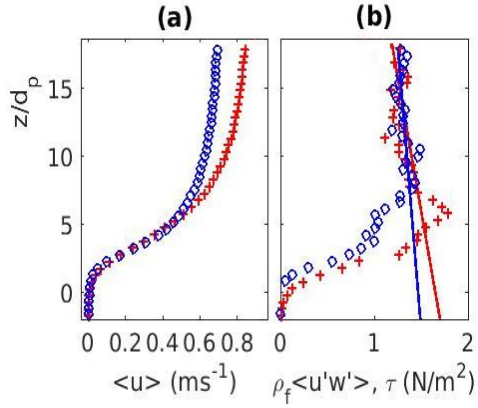

Figure 5: Mean profiles of streamwise velocity (a) and Reynolds shear stress (b), for UB-MES (blue, o) and ACVP (red, +).

The Reynolds shear stress profiles presented in Figure 5b show very similar order of magnitude for the two systems. Both profiles from ACVP and UB-MES display a quasi-linear behavior, indicating the uniform flow. The friction velocity, estimated based on the extrapolated Reynolds shear stress up to the bed interface, was about u^*=4.1 cm/s for UB-MES and u^*=4.3 cm/s for ACVP, which shows a good agreement between the systems.

4.2 Reduction of Von Karman parameter in SF

Despite similarities with the clear water velocity distribution, the law of the wall cannot be directly applied in this flow conditions, as previously shown by [16]. One reason is the reduction of the von Karman parameter (equal to κ=0.41 in clear water) in sediment-laden flows. Figure 6a shows the mean velocity profile and Figure 6b displays the mixing length. The mixing length can be estimated as follows [15]:

$$l = \frac{\sqrt{\tau/\rho_m}}{\left|\frac{du}{dz}\right|} \qquad (3)$$

where ρ_m is the fluid specific mass, τ is the total shear stress obtained from the extrapolation of the Reynolds shear stress profile. The slope of the linear fitting of the mixing length provides information regarding the von Karman parameter, which was κ=0.25 for the UB-MES and κ=0.24 for the ACVP. Thus, a good agreement is observed between both systems with respect to the vertical structure of the flow.

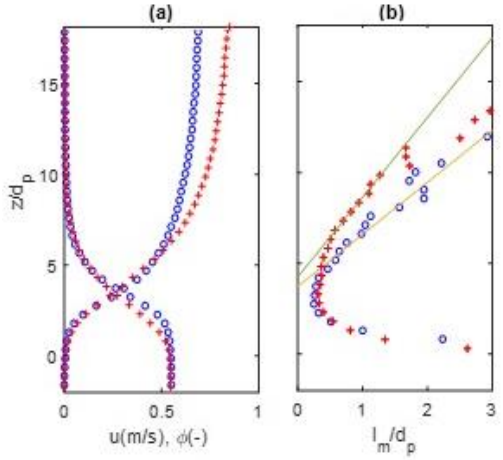

Figure 6: Mean velocity and concentration profiles (a) and mixing length (b); for UB-MES (blue, o) and ACVP(red, +).

4.3 Turbulent bursting events

Figure 7 presents the quadrant threshold distribution for the shear stress using H=0. Sweeps are the predominant events in the near-bed region. A similar behaviour is observed for UB-MES and ACVP. This is in agreement with [13] who argued that in hydraulically rough flows, sweeps dominate over ejections, and with [1], who describes sweeps as the governing mechanism for bed-mobility.

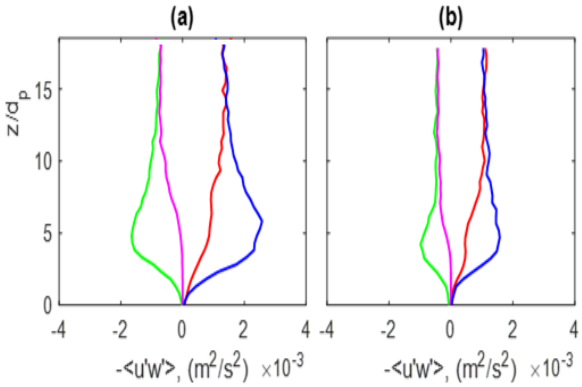

Figure 7: Quadrant threshold distribution for shear stress using H=0 for ACVP (a) and for UB-MES (b). blue=sweeps, red=Ejections, green=Outward interactions and purple=Inward interactions

As sweeps are the strongest events, it suggests that they are the most important for sediment suspension, as described by [5]. They reported that strong coherent structures are important contributors of suspended sediment transport, and that they carry a significant part of vertical sediment flux. The observed differences between CW and SF in terms of coherent flow structures are a clear evidence of turbulence modifications in sediment-laden flows.

6. Conclusion

In the present study, it was showed that UB-MES (prototype of the *UB-Lab 2C*) displays a good performance in high-resolution two components velocity profiling, by comparing its measurements with reference measurements from ACVP. The relative difference in measurements of both systems remained below 10% in CW and 20% in SF. Regarding the sheet-flow, differences in the flow conditions were observed between the two systems, explaining the greater relative differences compared with clear water conditions.

The capabilities of the *UB-Lab 2C* for time-resolved turbulence measurements are supported by similar results described in the literature, namely, the significant reduction of Von Karman parameter in sediment-laden flows and the higher contributions of ejections in CW (and sweeps in SF) for the Reynolds shear stress. This suggests the potential of this acoustic system to analyse a wide range of hydrodynamic phenomena, both in rigid-bed and mobile-bed, in which turbulence plays a major role.

Acknowledgment

The authors are grateful for the support of the French DGA through the ANR ASTRID program.

References

[1] Dey S, *Fluvial Hydrodynamics: Hydrodynamic and Sediment Transport Phenomena* (Springer Verlag Berlin Heidelberg), 2015.

[2] Dey, S., and R. Das, "Gravel-bed hydrodynamics: Double-averaging approach", *J. Hydraul. Eng*. 138(8), 707-725, 2012.

[3] Fromant, G., Mieras, R.S., Revil-Baudard, T., Puleo, J. A., Hurther, D. & Chauchat, J. "On bed load and suspended load measurement performances in sheet-flows using acoustic and conductivity profilers". *J. Geoph Res: Earth Surface*, 2018.

[4] Gust G and Southard J B, "Effects of weak bed load on the universal law of the wall". *J Geophys Res*, 88(C10):5939–5952, 1983

[5] Hurther D and Lemmin U, "Turbulent particle flux and momentum flux statistics in suspension flow", *Water Resour Res* 39(5):1139, 2003.

[6] Hurther D., Lemmin U. & Terray E.A., "Turbulent transport in the outer region of rough-wall open-channel flows: the contribution of large coherent shear structures", (LC3S) J. Fluid Mech., 574, 465-493, 2007.

[7] Hurther, D. & Thorne, P. D. "Suspension and near-bed load sediment transport processes above a migrating, sand-rippled bed under shoaling waves". J. Geophys. Res.: Oceans 116, C07001, 2011.

[8] Hurther D, Thorne P D, Bricault M, Lemmin U and Barnoud J M, "A multifrequency acoustic concentration and velocity profiler (ACVP) for boundary layer measurements of fine-scale flow and sediment transport processes", *Coastal Engineering*. 58, 594–605, 2011.

[9] Lu S S and Willmarth W W, "Measurements of the structure of the Reynolds stress in a turbulent boundary layer". *J. Fluid Mech.* 60, 481-511, 1973.

[10] Naqshband S, Ribberink J S, Hurther D and Hulscher S J M H. "Bed load and suspended load contributions to migrating sand dunes in equilibrium", *Journal of Geophysical Research: Earth Surface* pp. n/a–n/a. 2014.

[11] Nelson J, Shreve R L, McLean S R and Drake T G, "Role of near-bed turbulence structure in bed load transport and bed form mechanics", *Water Resour Res* 31,2071–2086, 1995.

[12] Nezu I Turbulent structure in open channel flow. PhD thesis, Kyoto University, Kyoto, 1977.

[13] Nezu I. and Nakagawa H, Turbulence in *Open-channel Flows*. (Rotterdam, Balkema), 1993.

[14] Nikora V I and Goring D G, "Effects of bed mobility on turbulence structure", *NIWA internal report* number 48, National Institute of Water & Atmospheric Research (NIWA), Christchurch, 1999.

[15] Prandtl, L. "Bericht über neuere Turbulenzforschung". Hydraulische Probleme pp. 1–13, 1926.

[16] Revil-Baudard T, Chauchat J, Hurther D. and Barraud P A, *Investigation of sheetflow processes based on novel acoustic high-resolution velocity and concentration measurements*. J. Fluid Mech. 767, 1–30, 2015.

[17] Revil-Baudard T, Chauchat J, Hurther D and Eiff O A, "Turbulence modifications induced by the bed mobility in intense sediment-laden flows"; *J. Fluid Mech.*, 808, 469 - 484. 2016.

[18] Thorne P D, Williams J J, Heathershaw A D, "In situ acoustic measurements of marine gravel threshold and transport", *Sedimentology* 36(1):61–74. 1989.